

PAPER

## MEH-PPV photophysics: insights from the influence of a nearby 2D quencher

To cite this article: Xuan Long Ho *et al* 2019 *Nanotechnology* **30** 065702

View the [article online](#) for updates and enhancements.



**IOP | ebooks™**

Bringing you innovative digital publishing with leading voices to create your essential collection of books in STEM research.

Start exploring the collection - download the first chapter of every title for free.

# MEH-PPV photophysics: insights from the influence of a nearby 2D quencher

Xuan Long Ho<sup>1</sup> , Yu-Han Wang<sup>2</sup>, Po-Jui Chen<sup>1</sup> , Wei-Yen Woon<sup>2,3</sup>  and Jonathon David White<sup>1,3</sup> 

<sup>1</sup>Dept of Electrical Engineering, Yuan Ze University, Chung-Li, Taoyuan City, Taiwan

<sup>2</sup>Department of Physics, National Central University, Jungli 32054, Taiwan

E-mail: [wymoon@phy.ncu.edu.tw](mailto:wymoon@phy.ncu.edu.tw) and [whitejd@xiaotu.ca](mailto:whitejd@xiaotu.ca)

Received 2 October 2018, revised 30 October 2018

Accepted for publication 15 November 2018

Published 11 December 2018



CrossMark

## Abstract

The effect of 2D quenching on single chain photophysics was investigated by spin coating 13 nm thick films of polystyrene lightly doped with MEH-PPV onto CVD grown graphene and observing the changes in several photoluminescent (PL) observables. With 99% of the PL quenched, we found a 60% drop in the PL lifetime, along with a significant blue-shift of the PL emission due to the preferential quenching of emission at longer wavelengths. During photo-bleaching, the blue spectral shift observed for isolated polymers was eliminated in the presence of the quencher up until 70% of the polymer was photo-bleached. Results were interpreted using a static disorder induced conjugation length distribution model. The quencher, by opening up a new non-radiative decay channel, ensures that excitons do not have sufficient time to migrate to nearby lower energy chromophores. The reduction of energy transfer into the lowest-energy chromophores thus reduces their rate of photo-bleaching. Finally, the difference between the quenched and non-quenched spectra allows the rate of energy transfer along the polymer backbone to be estimated at  $\sim 2 \text{ ns}^{-1}$ .

Keywords: conjugated polymers, photophysics, graphene, fluorescence quenching, photo-bleaching, fluorescence lifetime, single molecules

(Some figures may appear in colour only in the online journal)

## 1. Introduction

MEH-PPV (poly[2-methoxy-5-((20-ethylhexyl)oxy)-1,4-phenylene-vinylene]) is arguably the most studied conjugated polymer with over 1000 papers published in the year 2017 alone. Studies range from papers incorporating MEH-PPV into thin films for photovoltaic [1] and light emitting devices [2], to single molecule studies into the absorption and quantum yield of isolated MEH-PPV polymers embedded in inert optical matrices [3] and exciton–exciton annihilation (EEA) in single molecule aggregates [4]. It is quite amazing that despite 20 years of single molecule research, there is still much to learn about MEH-PPV photophysics.

That said, a general picture of the polymer has emerged and a consensus regarding the interplay between conformation and energy transfer emerged (see [4] or [5]). The long

chain polymer can be regarded as a collection of chromophores (oligomers) of various conjugation lengths that can both absorb and emit light [6]. Shorter chromophores absorb and emit at shorter wavelengths and more highly conjugated or longer chromophores emit at longer wavelengths. When this polymer is embedded in an inert (optically) matrix or in solution, it coils back on itself to form a defect-cylinder shape [7]—the persistence length playing a key role in determining the length of the cylinder. Upon low power excitation with light, an exciton is formed ( $\sim 5 \text{ nm}$  delocalization length) at an individual chromophore within the polymer. This exciton can either recombine at the same chromophore emitting light, or diffuse to a lower energy chromophore. Where chains are extended, excitons can only hop along the chain (intrachain exciton migration) while in areas which chains are coiled and adjacent chains are in close proximity (separation  $< 5 \text{ nm}$ ), excitons are free to jump between adjacent segments (inter-chain exciton migration). In the latter case, interchain exciton

<sup>3</sup> Authors to whom any correspondence should be addressed.

migration is generally orders of magnitude faster than intrachain energy transfer (generally quite slow) in the MEH-PPV system [8]. (A detailed study of the dependence of the rate of interchain energy transfer on chain separation has recently been published by Vanden Bout's group [9]). Thus, many papers talk of an energy funnel in tightly packed regions in which all energy is transferred to a single site and then emitted. To summarize, the conformation of the polymer determines energy landscape, energy transfer within and hence fluorescence emitted by MEH-PPV. This conformation is strongly affected by molecular weight [10], solvents [11], matrices, and sample preparation [12]. For example, when the solvent is chloroform, extended chains dominate the photo-physics while for solvents such as toluene, it is the emission from tightly packed regions that dominate.

The effects of conformation are most obvious in the fluorescence time trace observed in single molecule experiments as individual polymers photobleach. In the case of the extended chains, the time trace smoothly decays as the polymer photo-bleaches since there are numerous absorbing and emitting chromophores while in the case of tightly packed chains, frequent drops and jumps are visible as there are vastly fewer emitters. Another piece has recently been added to our understanding of photo-bleaching by Orritz's group [3]—Photoinduced traps and defects formed under prolonged illumination not only lead to a decrease in fluorescence but also to decreased absorption. In other words, once a chromophore is disabled, it can neither absorb or emit light.

In the work presented here we investigate changes to MEH-PPV photophysics brought on by this quenching of fluorescence by a nearby external quencher (graphene) and seek to use this information to understand the rate of intrachain energy transfer. In general, for a three-dimensional system, with point source emitters and accepters, energy transfer (and thus quenching) is subject to the standard FRET law:  $T(d) \sim (d_0/d)^6$  where  $d_0$  is the Forster Radius which is in the order of 6–10 nm for small molecules. As these distances are much smaller than the hydroscopic radius of MEH-PPV, quenching will have different effects on different parts of the molecule making any data analysis difficult. However in proximity to a 2D material such as graphene, a reduction in the exponent of the standard FRET law from 6 to 4 leads to a greatly extended quenching distance to up to 30 nm. This was predicted theoretically by Swathi in 2009 [13], and convincingly demonstrated experimentally by Federspiel in 2015 [14]. While interesting from a theoretical point of view, Kim *et al*, [15] demonstrated a practical application of this increased quenching distance: distinguishing between single and multilayer graphene by spin coating dye molecules over graphene separated by a 20 nm spacer of optically inert PMMA. Contrast was obtained from differences in the fluorescence intensity of the dye molecules. (Without the 20 nm spacer layer quenching was close to 100% for both single and multilayer graphene) While this quenching of fluorescence can be used to probe non-fluorescent 2D materials, this change in length scale allows a surface to be used to investigate the photophysics of the fluorescent molecules themselves. This is especially true for larger polymers such as

MEH-PPV as the effective distance for quenching now exceeds the hydroscopic radius of these large complicated molecules.

(An alternative to the usage of graphene would be a solid metal substrate. We have chosen to use graphene for three reasons. Firstly, graphene has been shown to be a more efficient quencher for fluorescent molecules, as compared with metals. [16] Secondly, in metal films, the excitation rate is altered via changes in the local strength of the electrical field and may be enhanced by several orders of magnitude [17]. Finally, in the distance domain relevant to this experiment (a few nanometers up to  $\sim 20$  nm), in the case of a metal film, a significant fraction of the excited fluorescence couples back to surface plasmon polaritons by fulfilling momentum matching conditions. This represents a significant loss of fluorescence yield. [17]. Using graphene avoids or at least greatly reduces these complications. [16])

Previous work, such as that undertaken by the groups of Bardeen [18] and Mingqiang Wang [19], involving graphene to probe MEH-PPV has focused reduced graphene-oxide (rGO)/MEH-PPV composite films. While both these groups observed strong quenching of fluorescence, the first group found that the fluorescence lifetime decreased an order of magnitude as the rGO component increased while the second group did not observe any change in lifetime for their sample suggesting that the quenching mechanism is strongly dependent on preparation of the MEH-PPV films. These investigations of thin films, in which 3D energy transfer dominates, is quite a different domain than in an extended single molecule where 1D intrachain is the dominate energy transfer mechanism. In general for single fluorophores, on CVD grown graphene, the quenching mechanism is the non-radiative decay of the fluorophore—not charge transfer, except for those chromophores in close (sub-nm) proximity to the graphene interface [16].

This paper is organized as follows: the experimental procedures used are elucidated, the data is then presented with minimal comment. After the presentation of all the data, the results are interpreted in terms of the molecular exciton model [6] involving polymers composed of loosely and tightly coiled segments. Throughout paper, we distinguish between photo-bleaching (permanent changes to the chemistry of MEH-PPV primarily due to interaction with oxygen) resulting in reduced absorption and photoluminescence, and quenching due to the presence of nearby molecules to which energy is transferred (either by exciton migration, hole/electron charge separation, whether resonant or non-resonant energy transfer [20]). In this context, a quencher does not affect the chemistry of MEH-PPV and quenching disappears if/when the quencher is removed.

## 2. Experiment

Monolayer graphene was grown on 25  $\mu\text{m}$  thick copper foil in a quartz tube furnace system using CVD [21]. Under vacuum conditions of 10 mTorr and at a temperature of 1000  $^\circ\text{C}$ , hydrogen was first introduced (flow rate = 2 sccm) for 40 min,

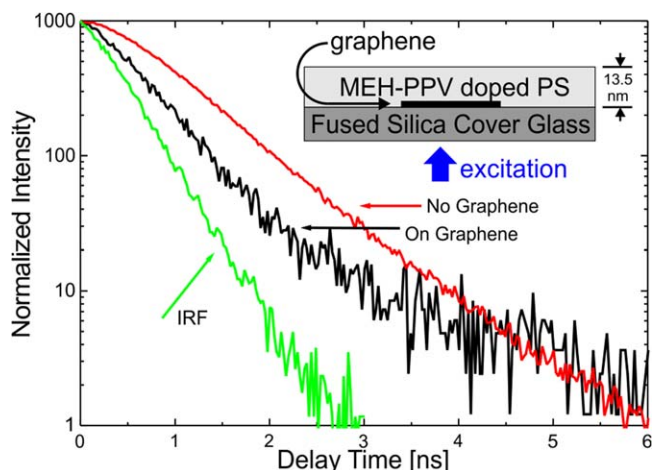


**Figure 1.** Ensemble averaged fluorescence decay time for MEH-PPV polymers with (black line) and without (red line) graphene present. The green line is the instrument response function of our system. All curves are normalized to 1000. [inset] Schematic of the device structure used indicating direction of excitation.

followed by methane (35 sccm) for 15 min quick cooling was then applied ( $300\text{ }^{\circ}\text{C min}^{-1}$ ) under continuous methane and hydrogen gas flows. A layer of polymethylmethacrylate (PMMA) was then spin-coated onto the as-grown films. The PMMA/graphene film was separated from the Cu substrate by a bubble-free electrochemical delamination transfer protocol [22]. Finally, films were transferred to  $100\text{ }\mu\text{m}$  thick, UV cover glass (Esco Optics), and the PMMA was dissolved with acetone. The graphene film's monolayer characteristics and film quality were verified using micro-Raman spectroscopy. Films exhibited the characteristic monolayer signature ( $I_{2D}/I_G \sim 2$  and symmetric 2D band).

MEH-PPV (Aldrich,  $M_n = 150\text{--}250\text{ kD}$ ) was first mixed with polystyrene (PS, Fluka,  $M_w = 184\text{ kD}$ ,  $M_n = 178\text{ kD}$ ) at a ratios of 1.0 wt%, 0.1 wt%, and 0.01 wt% and dissolved in 1-Chloropentane (Acros,  $2\text{ mg ml}^{-1}$ ). Low concentrations were chosen to ensure the fluorophores were well separated and that the probability of multi-polymer aggregate or dimer formation was negligible. 1-Chloropentane's low vapor pressure allows very uniform and smooth thin films to be spin-coated [23]. After mixing for 7 days at 300 K and filtering ( $0.45\text{ }\mu\text{m}$ ), the solution was spin-coated onto the graphene coated UV cover glass to form a  $t = 13.5 \pm 1.5\text{ nm}$  (as measured by AFM) thick PS film containing the well separated MEH-PPV molecules. Films were dried under vacuum conditions for 2 d at room temperature to remove remaining solvent. Figure 1(inset) illustrates the devices structure.

Samples were observed using our home built vacuum confocal microscope [24]. Excitation light was focused through the cover glass and graphene layer onto the MEH-PPV polymers using a 60x,  $\text{NA} = 0.85$  objective lens (Nikon). PL was collected through the same objective lens (epifluorescence mode), and after appropriate filters (passing  $\lambda > 500\text{ nm}$ ), focused by an  $f = 200\text{ mm}$  doublet lens into a  $\varphi = 100\text{ }\mu\text{m}$  optical fiber. During spectral measurements, a piezo-electric stage (Physic Instruments) scanned the sample over an area of  $30 \times 30\text{ }\mu\text{m}^2$ , (pixel frequency of 100 Hz,

step size of  $1\text{ }\mu\text{m}/\text{pixel}$ ) to average over an ensemble of fluorophores and to avoid photo-bleaching.

For lifetime measurements, 5 ps (FWHM),  $\lambda_{\text{excite}} = 466\text{ nm}$  (FWHM = 6 nm) pulses at 10 Mhz (PicoQuant, PDL 800-B laser driver with (PicoQuant LDH-P-C-470 laser head) were used for excitation. A maximum excitation fluence of  $\sim 80\text{ nJ}/\text{cm}^2/\text{pulse}$  was chosen to ensure that nonlinear effects such as EEA were minimal [4]. The optical fiber collecting the light was directed to an SPCM avalanche photodiode (Perkin-Elmer) connected to a time-correlated single-photon counting card (SPC 630, Becker and Hickl). The instrument response function (IRF) was deconvoluted out of the measurements and the lifetime data was fit using SPCimage (Becker and Hickl). Data was analyzed using double-exponential FRET as prescribed by Becker [25] where possible.

Survival time of the isolated polymers was taken using the same laser employed in the lifetime measurements but at a lower average power ( $1\text{ }\mu\text{W}$ ,  $100\text{ W cm}^{-2}$ ). For these measurements the piezo-electric stage was used only to focus on the isolated MEH-PPV polymers (i.e. no scanning was involved during the taking of data). In order to observe changes in spectral composition during the decay, PL was split by a dichroic beamsplitter ( $\lambda = 560\text{ nm}$ ) and the decay in intensity of the long and short wavelength components observed by separate APDs. The signal on both channels were well fit by three-exponential decay:

$$I(t) = \sum_{i=1}^{i=3} A_i e^{-\frac{t}{\tau_i}}. \quad (1)$$

Based on the multi-exponential curve fit, the mean survival time was determined:

$$T_{\text{mean}} = \frac{\sum_{i=1}^{i=3} A_i \tau_i}{\sum_{i=1}^{i=3} A_i}. \quad (2)$$

The ratio between the two channels intensity during photo-bleaching was analyzed using the spectral shift coefficient ( $S$ ) [26], defined as:

$$S(t) = \frac{I(t, \lambda > 560\text{ nm}) - I(t, \lambda < 560\text{ nm})}{I(t, \lambda > 560\text{ nm}) + I(t, \lambda < 560\text{ nm})}. \quad (3)$$

An increasingly value of  $S$  indicates a gradually reddening of the spectra while a decreasing value suggests the spectrum is increasingly dominated by shorter wavelength components.

### 3. Results

Figure 2 presents the ensemble MEH-PPV PL spectrum before photo-bleaching inside and outside the graphene coated areas of the cover glass. Comparing the scales on (a) and d(b), it can be seen that  $\sim 99\%$  of the PL is quenched. This is consistent with the results of Kim [15] in which they found almost 100% quenching of fluorescence for dye layers thinner than 5 nm. As seen in figure 2 top in the absence of graphene, the PL spectrum is well fit by two peaks, one at

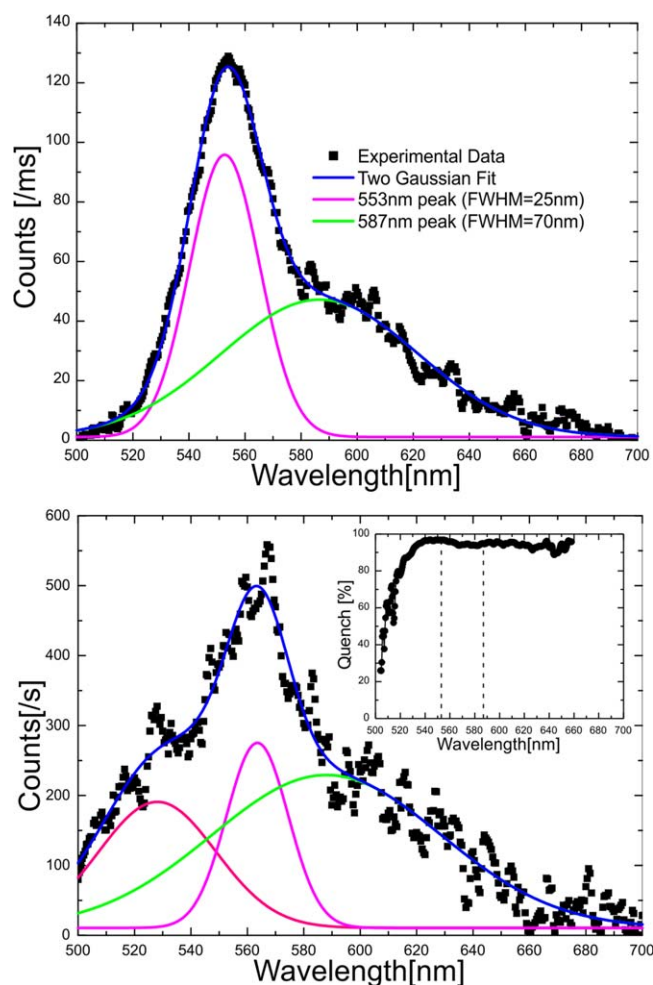


**Figure 2.** Photoluminescence spectrum of an ensemble of MEH-PPV polymers (top) without graphene and (bottom) in close proximity to graphene. Experiment data is presented as squares. The blue lines are the result of curve fitting with 2 (top) or 3 (bottom) Gaussian functions, respectively. Without graphene the spectra is well fit by two Gaussian peaks—one at 553 nm (FWHM = 25 nm) and one at 587 nm (FWHM = 70 nm). (bottom inset) Wavelength dependence of quenching of MEH-PPV fluorescence by graphene.

553 nm (FWHM = 25 nm) and the other at 587 nm (FWHM = 70 nm) representing the fundamental vibrational and the overlap of the 1st vibrational band of the extended chains with the fundamental vibrational band of the collapsed chains. The Huang-Rhys Factor of 0.26 indicates the dominant role that extended chains or ‘blue’ chromophores (rather than tightly packed or ‘red’ chromophores) play in the emission. We note that this spectrum is unchanged for doping concentrations <1%. In the presence of graphene (figure 2 *bottom*) the spectrum, in addition to being of low intensity, is severely distorted—no longer can the spectrum be fit by two or even three peaks. The main fundamental vibration band along with the overlap of the 1st vibrational band of the extended chains with the fundamental vibrational band of the collapsed chains still dominates the spectrum, but there are also considerable short wavelength components emitting from 540 to 500 nm (and slightly below as our filter only passed  $\lambda > 500$  nm). Figure 2 (*inset*) presents the

quenching efficiency with respect to wavelength. Quenching efficiency is approximately wavelength independent from 540 to 650 nm at over 95%. (Above 650 nm, our signal to noise ratio does not allow us to make any conclusions.) Below 540 nm; however, the quenching is much less efficient ranging from ~30% to 90%. The key point here is that in the quenched spectrum, there are no new sources of emission. Rather it is the short wavelength components (present in the original spectrum) become significant in the quenched spectrum.

Figure 1 presents the as-measured ensemble averaged fluorescence decay time for MEH-PPV polymers with and without graphene present. In the absence of the quencher purely single exponential decay can be seen for over 3 orders of magnitude. After taking into consideration the impulse response function (IRF) of our system, the fluorescence lifetime is ~900 ns. This is typical of values obtained in single molecule experiments for PPV derivative polymers [27, 28]. As can be seen in the figure, the PL lifetime shortens in the presence of the quencher indicating that graphene has opened up an additional non-radiative decay path for the excitons. The reduced lifetime indicates a dynamic quenching process. Lifetime reduction was independent of concentration for MEH-PPV doping ratios from 0.01% to 1% suggesting that intermolecule interactions are negligible at the concentrations employed in this experiment.

The lifetime decays were fit by 2 exponential decay curves with the mean lifetime of MEH-PPV on graphene being a factor of 3 shorter than for the pristine film (~300 versus ~900 ps). On occasion, the pristine MEH-PPV decay was clearly single exponential. In this case, in order to obtain more quantitative information about the nature and efficiency of energy transfer, we employed the double-exponential decay analysis technique [25] to gain additional insights into the quenching process. The results indicated in table 1.

In the absence of the quencher, there is only one component to the lifetime having a value of 910 ps which we identify as  $\tau_o$ .—The average lifetime of the noninteracting (unquenched) chromophores. For the film on graphene, the mean lifetime drops from 910 to 230 ps. Two components are evident in the lifetime decay, a fast lifetime component at  $220 \pm 60$  ps ( $\tau_{ET}$ ) from the interacting (quenched) chromophores, and the slow lifetime component at 910 ps ( $\tau_o$ )—due to the noninteracting (unquenched) chromophores. The shorter component dominates the process with the ratio of the two lifetimes (AET: Ao) being 99:1. According to the double-exponential decay analysis technique, this ratio represents the relative numbers of interacting and noninteracting chromophores. In other words, the vast majority (99%) of the chromophores in the MEH-PPV polymer are being quenched by the graphene (in good agreement with the intensity data).

The transient time traces of photoluminescence of an ensemble of MEH-PPV molecules under continuous excitation (top) in the absence of graphene and (middle) in close proximity to graphene as MEH-PPV photo-bleaches are presented in figure 3. The initial intensity without graphene is 2 orders of magnitude greater than in the presence of graphene. In the absence of graphene, the emission drops by 90%

**Table 1.** Lifetime fitting parameters.

Location	$\tau_1$ (ps)	$A_1$ (%)	$\tau_2$ (ps)	$A_2$ (%)	t(mean) (ps)
No Graphene	910	100	—	0	910
On Graphene	220	99	910	1	230

within 30 s. With graphene quenching the emission, photo-bleaching occurs on a much slower time scale—only dropping by about 44% in the first 30 s. It is only after 18 min that the intensity drops by 90%. This ‘protective effect’ of graphene has been previously reported by Mingqiang Wang’s group [19].

Fitting the transient time traces requires three exponential decay components. Table 2 presents the values of these parameters. Averaging over the whole spectrum, at the excitation power used here, the mean photo-bleaching time lengthens ten times in the presence of graphene (11  $\rightarrow$  107 s). The shortest time constants are all  $\sim$ 2 s. It seems the presence of graphene has little affect on this time constant. The middle time constant more than doubles in the presence of graphene (12  $\rightarrow$  29 s), and the longest time constants lengthens by a factor of 6 (68  $\rightarrow$  382 s) in the presence of graphene. The key difference between the two samples is the weighting of the various components—in the presence of graphene the weighting of the longest time component increases by a factor of four. In the pristine MEH-PPV film, the longest time component is only a minor contributor to the overall decay curve fit, while in the presence of graphene it takes on equal weight with the faster decay components.

As the sample slowly photo-bleaches the emission spectra gradually shifts. This is seen in the different time constants for the shorter (<560 nm) and long wave (>560 nm) components (table 2) In the absence of graphene, the long wavelength emission decays with a mean time that is less than half of that of the shorter wavelength components resulting in a continuous spectral blue shift with time. This is seen clearly in figure 3(top)—right axis—where we have plotted the spectral shift as a function of the log of time. This continuous blue shift is consistent with that observed by Liang for MEH-PPV [26].

Vastly different behavior is seen in presence of the graphene. As seen in figure 3 (middle) (right axis), the spectral shift changes little over time. Initially more blue than the pristine MEH-PPV due to the preferential quenching of the longer wavelength components (see figure 2 (inset)), during the first 100 s despite a drop in intensity of 70%, the spectra only slightly red-shifts by 0.05. After 100 s the spectral shift reverses and as the spectrum gradually shifts towards the blue. For the first  $\sim$ 30 s, as the intensity drops 50%, the rate of change is linear on a log scale. After 30 s the spectrum starts to shift blue again following a quadratic equation. Overall the Spectral Coefficient only changes by 0.1 as PL emission drops 90%—in stark contrast to the change of 0.35 observed for unquenched MEH-PPV. This spectral robustness is reflected in the fact that all three time constants are similar for the short and long wavelength components. We note that similar behavior was observed by Liang but only for short

chain rod-like polymers (DOO-PPV) in which there is very limited energy transfer between chromophores along the polymer backbone [26].

The bottom pane of figure 3 presents the change in spectral coefficient ( $S$ ) with the percent of the polymer that has been photo-bleached. In the absence of graphene, the spectra continuously blueshifts as the polymer photo-bleaches. The rate of blue-shifting is linear with percent bleached until about 90% bleaching. In contrast, in the presence of graphene, the spectra only starts to blue-shift after  $\sim$ 60% of the polymer has been photo-bleached and becomes pronounced only after 80% of the polymer has been photo-bleached.

A series of films were prepared with different concentrations of MEH-PPV to check for any concentration dependent artifacts. Results were independent of concentration below 1% while above 5% interchain effects such as aggregation involving more than one polymer become significant—as evidenced by a significant change in PL spectra. As the purpose of this work was to study energy transfer and quenching in well separated extended chains where the slower intrachain energy transfer dominates, we worked well below this critical concentration. Results were consistent and within experimental error over three orders of magnitude of MEH-PPV concentration as seen in table 3 where we have presented the percent quench and mean lifetime. (Note that the concentrations listed are nominal MEH-PPV concentrations prior to filtration, so the final concentrations are presumably lower).

It is also interesting to verify the efficiency of quenching with film thickness. In order to do this, a series of tri-layer films were prepared including a PMMA spacer layer between the graphene sheet and the MEH-PPV doped film following the method of [23, 29]. The thickness of the PS matrix layer containing MEH-PPV was kept constant at 13.5 nm. Figure 4 presents the results obtained for quenching and mean survival time as a function of the thickness of the spacer layer. As can be seen in figure 4, graphene successfully quenches emission resulting in an enhanced survival time for spacer layer thicknesses up to 20 nm or total thicknesses of about 35 nm. At distances greater than 60 nm, graphene has no effect on the emission characteristics of the polymer.

#### 4. Discussion

This data can be understood in terms of the molecular exciton model in which the polymer is considered to be composed of different conjugated segments. This model has been used to explain the chain-length dependence of the absorption and third-order nonlinear susceptibilities of the well-defined linear

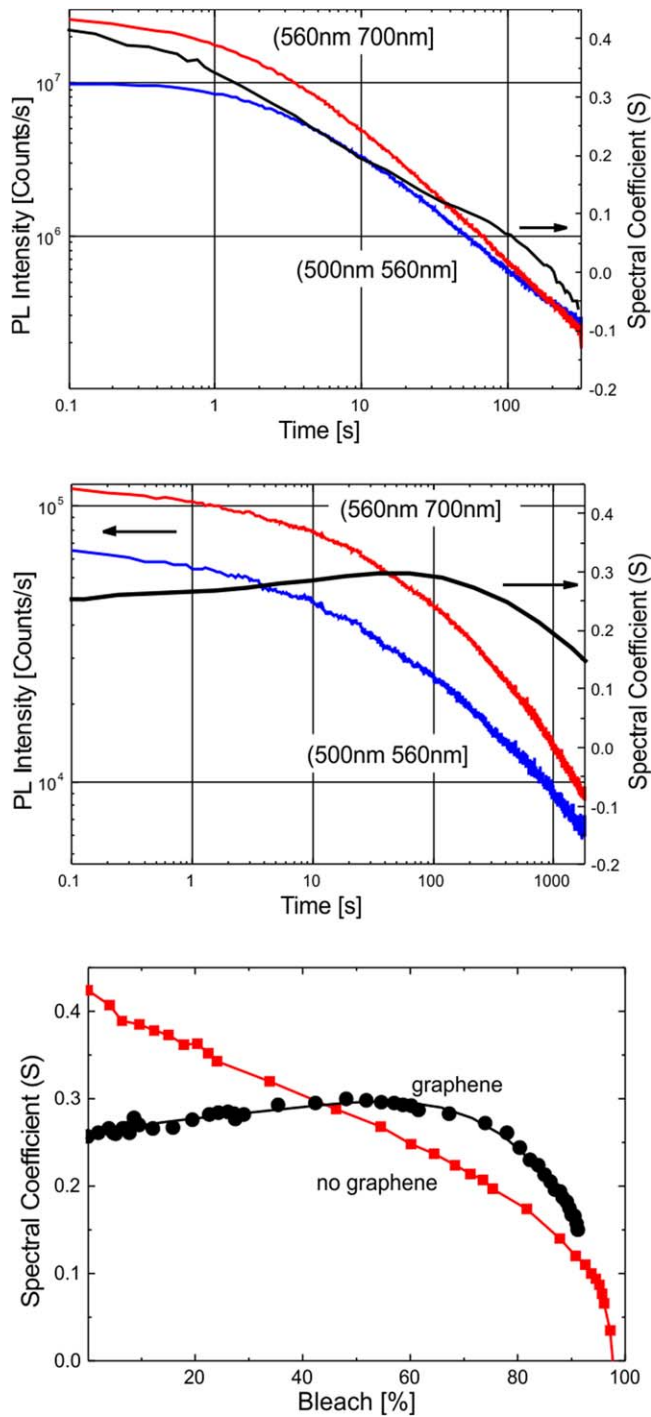


**Figure 3.** Transient time traces of photoluminescence of an ensemble of MEH-PPV molecules under continuous excitation with 466 nm laser light. (top) without graphene (middle) in close proximity to graphene. Red lines represent the emission at wavelengths  $>560$  nm while the blue lines present the emission at  $<560$  nm. The average power on the sample was  $1 \mu\text{W}$ . Black lines represent the change in spectral coefficient as the sample photo-bleaches. (right axis) (bottom) Change in spectral coefficient ( $S$ ) as a function of the percent of polymer bleached in the presence or absence of the graphene underlayer.

polyene oligomers [30], as well as the steady-state absorption and PL spectrum of PPV derivatives in solution [6] and in solid solution [27, 31]. This phenomenological treatment is suitable for understanding long time ( $>100$  ps) photophysics

processes—the time regime in which this experiment was performed. In this model (see [6] for details) the appearance of different conjugated segments is governed by a distribution function.

$$D[N] = \frac{1}{\pi\sigma} \exp\left[-\frac{N - N_o}{\sigma^2}\right], \quad (5)$$

where  $N$  is the length of the conjugated segment.  $D[N]$ , calculated based on a conformational disorder model [32], denotes the probability of finding an oligomer having  $N$ -units in the chain. (Parameters  $N_o \sim 5$  and  $\sigma \sim 1.8$  are determined experimentally).

The absorption coefficient of a polymer is expressed as the sum of the absorptions of its component oligomers  $\alpha_i(\omega)$ :

$$\alpha(\omega) = \sum_i \alpha_i(\omega) = \sum_N D[N] \alpha_N(\omega), \quad (6)$$

where  $\alpha_N(\omega)$  represents the absorption spectrum of an  $N$ -unit conjugated segment (oligomer or alternatively chromophore). The longer the conjugation length, the smaller the energy gap—and thus absorption and emission become progressively red-shifted as the conjugation length increases until the effect saturates for conjugation lengths greater than  $N = 9$ . The intensity of the PL spectrum is expressed as:

$$I(\omega) = \sum_i I_i(\omega) = \sum_N \rho[N] D[N] PL_N(\omega), \quad (7)$$

where  $I_i(\omega)$  is the PL emission spectra for the  $i$ th oligomer and then summed over all oligomers in the chain,  $PL_N(\omega)$  is the area normalized PL spectrum for an oligomer of length  $N$ , and  $\rho[N]$  represents the relative weighting of each occurring oligomer's contribution to the PL spectrum. In the original model, which was applied in solution, it was assumed that thermal equilibrium was reached between all electronic states prior to emission, i.e. rapid energy transfer ( $k_{\text{inter}}$  and  $k_{\text{intra}} < 50$  ps). Later work has shown that this is not a valid assumption for single molecules embedded in solid solutions since energy transfer along the polymer backbone is not extremely rapid relative to fluorescence lifetime. [8, 26, 31, 33] (The question of how slow this energy transfer rate has not been adequately addressed and is one focus of this paper).

As such, in figure 5(a) we present a revised generalized schematic illustrating energy transfer in MEH-PPV based on a molecular exciton model in which the energy transfer rates are explicitly considered. Considering first, the polymer in the absence of a quencher. An oligomer of length  $N$  can be excited directly by absorbing light or indirectly by energy transfer from a nearby shorter oligomer. Once excited, besides returning to the ground state via non-radiative decay (with between 90% [3] and 50% [27] probability, not shown explicitly in the diagram), the oligomer may either emit light (with rate  $k_r$  of the order of  $1 \text{ (ns}^{-1}\text{)}$  [27, 28]) or the exciton may diffuse to a nearby longer oligomer. The energy transfer from one oligomer to another may occur either by interchain energy transfer ( $k_{\text{inter}}$ )—the through-space Forster transfer (FRET) between two polymer segments that are in close proximity— or intrachain energy transfer ( $k_{\text{intra}}$ )—energy transfer between two neighboring segments along the backbone of a single polymer chain. Due to the fact the transition

**Table 2.** Survival time fitting parameters.

Sample	Wavelength	$T_{\text{mean}}$ (s)	$\tau_1$ (s)	$\tau_2$ (s)	$\tau_3$ (s)	$A_1/A_2$	$A_3/A_2$
Pristine (no graphene)	$\lambda < 560$ nm	16	3.0	16	81	0.6	0.3
	$\lambda > 560$ nm	6.2	1.5	8	55	0.3	0.2
	All	11	2.3	12	68		
On graphene	$\lambda < 560$ nm	97	1.8	26	379	0.7	0.8
	$\lambda > 560$ nm	116	1.9	31	385	0.6	1.0
	All $\lambda$	107	1.9	29	382		

**Table 3.** Concentration dependence of quenching and lifetime.

MEH-PPV (%)	% Quench (%)	Mean lifetime (s)	
		No graphene	Graphene
0.01	96% $\pm$ 3%	0.93 $\pm$ 0.1	0.24 $\pm$ 0.1
0.1	99% $\pm$ 3%	0.82 $\pm$ 0.1	0.25 $\pm$ 0.1
1.0	99% $\pm$ 3%	0.98 $\pm$ 0.1	0.39 $\pm$ 0.1

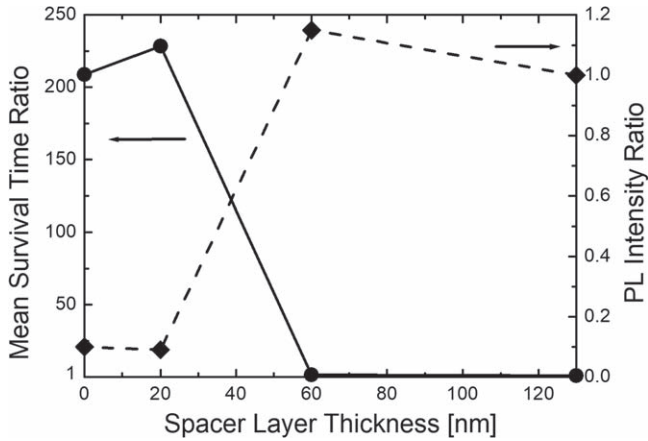


**Figure 4.** Effect of spacer layer thickness on quenching and mean survival time. The structure is composed of glass/graphene/PMMA (various thicknesses)/0.01% MEH-PPV embedded in a 13.5 nm thick polystyrene matrix. The left axis presents the ratio of survival time with and without graphene as a function of the thickness of the spacer layer (circles, solid line) while the right axis presents the corresponding the intensity ratio (diamonds, dashed line).

dipoles of MEH-PPV are along the polymer's backbone, intrachain energy transfer via Förster transfer is inherently weak and thus  $k_{\text{intra}} \ll k_{\text{inter}}$ . Work by Schwartz's groups suggests that  $k_{\text{inter}}$  is in the order of 1 (ps<sup>-1</sup>) [33]. This results in 'energy funnels' and red chromophores discussed in many papers [3, 26], in which energy transfers transfer to a single emitter in an area of the polymer where the chains are tightly coiled. The existence of this pathway is seen in the transients of single molecules where a single photo-bleaching event leads to a sudden drop in emission intensity [34]. As our sample is comprised of mainly extended loosely packed chains, we do not include interchain energy transfer in our equations. As a result we can express change in population of

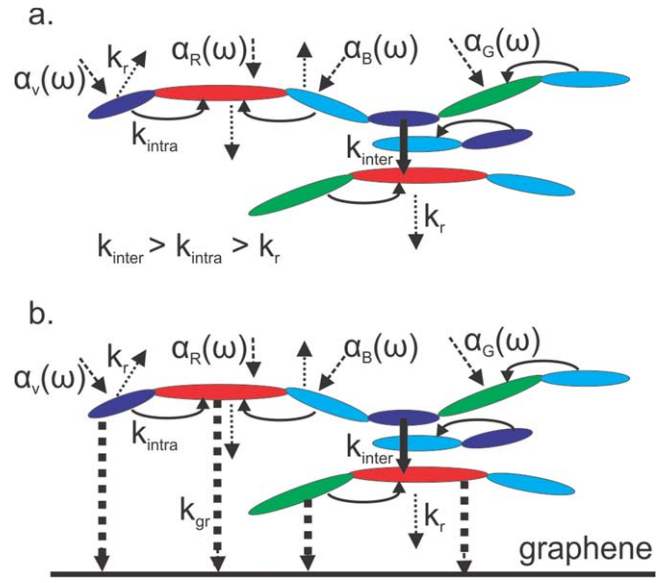


**Figure 5.** Generalized schematic illustrating energy transfer in MEH-PPV based on a molecular exciton model. (a) without graphene (b) in close proximity to graphene. Alpha represents the absorption of an oligomer of length  $N$  at the excitation frequency. Dotted arrows represent radiative decay channels with rate  $k_r$ , curved lines represent intrachain energy transfer channels with rate  $k_{\text{intra}}$ , thick solid lines represent interchain energy transfer with rate  $k_{\text{inter}}$ , and the thick dashed line represents energy transfer to graphene with rate  $k_{\text{gr}}$ .

the singlet excitation state of the  $i$ th oligomer ( $S_1^i$ ) as:

$$\frac{dS_1^i}{dt} = k_{\text{abs},n_i} S_0^i - (k_r + k_{nr}) S_1^i + \sum_{j=i-1}^{j=i+1} (k_{\text{intra}} S_1^j \delta_{n_i > n_j} - k_{\text{intra}} S_1^i \delta_{n_i < n_j}), \quad (8)$$

where  $n_j$  is the conjugation length of the  $j$ th oligomer,  $\delta_{n_i < n_j}$  is 1 if the conjugation length of the  $i$ th oligomer is less than the  $j$ th oligomer and zero otherwise.  $k_{\text{abs},n_i} = I(\omega_{\text{ex}}) \alpha_{n_i}(\omega_{\text{ex}})$  is the rate of excitation of the  $i$ th oligomer.  $S_0^i$  and  $S_1^i$  represent the population of the ground and excitation state, respectively. The first term reflects the direct excitation of the  $i$ th oligomer by the excitation light and is proportional to both intensity and absorption. The second term represents the return to the ground state via radiative ( $k_r$ ) and non-radiative transitions ( $k_{nr}$ ). The final terms represent energy transfer or exciton migration from (to) adjacent oligomers of shorter (longer)

conjugation length. Note that we have ignored energy transfer to the triplet state. Under cw illumination, the excited state population of the  $i$ th oligomer is given as:

$$S_i^i = \frac{1}{k_r + k_{nr}} \left( k_{absp,n_i} S_0^i + \sum_{j=i+1}^{j=i+1} (k_{intra} S_1^j \delta_{n_i > n_j} - k_{intra} S_1^i \delta_{n_i < n_j}) \right). \quad (9)$$

The solution involves solving the 1000 coupled equations individually. The contribution to emission from the  $i$ th oligomer to the total emission is:

$$I_i(\omega) = k_r S_1^i PL_{n_i}(\omega). \quad (10)$$

The total PL emission is thus found using equation (7). We have assumed that the intrachain energy transfer rate is independent of oligomer length as a first approximation.

A photo-bleaching event occurs when an excited oligomer in the triplet state comes into contact with triplet oxygen. The dynamics of the conversion from the directly excited singlet to triplet exciton ( $S_1 \rightarrow T_1$ ) in MEH-PPV has been studied extensively [35, 36] and the intersystem crossing rate ( $k_{isc}$ ) shown to be of the order of  $k_{isc} = 10 \text{ ms}^{-1}$  [36]. Upon reaction of the triplet state of MEH-PPV with oxygen, the resulting chemical changes result in the cessation of not only emission but also, as recently shown by Orrit's group [3], absorption at the bleached site. The effect of a photo-bleaching event on nearby oligomers depends on whether interchain or intrachain energy transfer dominates. In the case of the energy funnel (interchain energy transfer), there is no disruption of energy transfer to the bleached chromophore. This is reflected in a sudden drop in emission intensity [34]. Completely different behavior is seen in the loosely coiled regions where intrachain energy transfer dominates. In this case, the system acts like a traditional donor-accepter system in which the donor starts to emit light once the acceptor is quenched. [10, 28]. In the presence of photo-bleaching events, equation (9) for the extended chain is then modified as:

$$S_1^i = \frac{1}{k_r + k_{nr}} \left( \delta_{bl,i} k_{absp,n_i} S_0^i + \sum_{j=i-1}^{j=i+1} \delta_{bl,j} (k_{intra} S_1^j \delta_{n_i > n_j} - k_{intra} S_1^i \delta_{n_i < n_j}) \right), \quad (11)$$

where  $\delta_{bl,j} = 1$  if the  $j$ th oligomer has not been photo-bleached. This equation reflects the inability of a bleached oligomer to directly absorb light or receive energy from neighboring oligomers via intrachain energy transfer. The probability of a photo-bleaching event depends on the availability of oxygen, as well as the amount of time an oligomer spends in the excited state [37]. Thus one expects that oligomers which are excited indirectly via energy transfer in addition to direct excitation will bleach first.

As an example, consider the simplest case: that of a polymer containing only two oligomers. Solving analytically (assuming oligomer 1 is longer than oligomer 2):

$$S_1^2 = \delta_{bl,2} \frac{k_{absp,n_2} S_0^2}{k_r + k_{nr} + \delta_{bl,1} k_{intra}} \quad (12a)$$

and

$$S_1^1 = \frac{\delta_{bl,1}}{k_r + k_{nr}} (k_{absp,n_1} S_0^1 + \delta_{bl,2} k_{intra} S_1^2) = \frac{\delta_{bl,1}}{k_r + k_{nr}} \left( k_{absp,n_1} S_0^1 + \delta_{bl,2} k_{intra} \frac{k_{absp,n_2} S_0^2}{k_r + k_{nr} + k_{intra}} \right). \quad (12b)$$

Experimentally, changes in emitters and energy transfer due to gradual photo-bleaching of the MEH-PPV are reflected in the spectral components of the transient time trace (figure 3). Two distinct cases can be considered:  $k_{intra} \ll (k_r + k_{nr})$  and  $k_{intra} > (k_r + k_{nr})$ . In the first case, emission is dominated by the direct fluorescence of the absorbing oligomer—energy transfer from adjacent oligomers does not play a role as excitons recombine before they have a chance to migrate to an adjacent oligomer. Thus the relative length of time an oligomer spends in the excited state, and hence probability of being photo-bleached is solely dependent on the oligomer's absorption coefficient relative to the other oligomers in the long chain polymer. In terms of the transient time trace, while the intensity drops greatly, spectral change is thus expected to be minimal during photo-bleaching. The direction of the shift (towards longer or shorter wavelengths) will be controlled by the relative absorption coefficient at the excitation wavelength of the various oligomers. Turning now to the second case, in which intrachain energy transfer occurs on a time scale that is shorter than the fluorescence lifetime. The probability of an oligomer being in an excited state is correlated with the length of the oligomer. For the shortest oligomers, excitons only diffuse away to its neighbors decreasing the probability of finding it in the excited state, while for the longer oligomers, excitons diffuse from its neighbors increasing this probability (see equation (9)). Thus the probability of photo-bleaching is higher the longer the oligomer. In addition, once the longer accepters are bleached, adjacent shorter oligomers which were previously transferring energy to these longer segments start to emit more strongly [10, 28]. Both of these effects will result in a spectra that continuously blue shifting as photo-bleaching occurs. The continuous blue-shift of spectrum in figure 3(bottom) for MEH-PPV indicates clearly that longer oligomers are bleaching first and thus are spending more time in the excited state—in other words,  $k_{intra} > (k_r + k_{nr})$ .

The effect of quenching is to open an additional non-radiative decay channel (see figure 5(b)) to graphene. This can be represented either by incorporating the graphene quenching rate ( $k_{gr}$ ) directly into the non-radiative decay rate or by modifying equation (8) by adding an additional relaxation rate  $k_{gr}$  to explicitly include energy transfer from the polymer to graphene. Based on our measurement of the fluorescence lifetime ( $\tau_f = 1/(k_r + k_{nr})$ ) and the values for

decay rates in closely related DO-PPV [27],  $k_r = 0.58 \text{ ns}^{-1}$ ,  $k_{nr} = 0.5 \text{ ns}^{-1}$ , and our estimate for  $k_{gr} = 4.3 \text{ ns}^{-1}$ , based on  $\tau_{\text{ET}}$ , we have chosen explicitly to write the effect of graphene as this rate dominates both the radiative decay rate and the other non-radiative decay channels. That is we replace  $(k_r + k_{nr}) \rightarrow (k_r + k_{nr} + k_{gr})$

Turning our attention now to figure 3(middle) and figure 5(b), it can be seen that in the presence of graphene, the continuous blue-shift with photo-bleaching of MEH-PPV has been arrested. Up until 60% of the polymer is bleached, the spectra shifts slightly towards the red and not towards the blue. This clearly indicates that longer oligomers are not spending more time than shorter oligomers in the excited state, but rather the relative absorption coefficients of the oligomers playing the key role. In other words, limited energy transfer ( $k_{intra} \ll (k_r + k_{nr} + k_{gr})$ ). Combining the results with and without the quencher, allows us to put limits on the rate of intrachain energy transfer in MEH-PPV:  $(k_r + k_{nr}) < k_{intra} \ll (k_r + k_{nr} + k_{gr})$ . Substituting in the mean fluorescent lifetimes measured earlier suggests that the rate of intrachain exciton migration is within the range  $0.9 \text{ ns}^{-1} < k_{intra} < 3.3 \text{ ns}^{-1}$ .

Finally we turn to the wavelength dependence of quenching (before photo-bleaching, as seen in figure 2(inset)). In the absence of the quencher, the shortest conjugated segments make only a small contribution to total PL since (1) their absorption is relatively small compared to longer segments and (2) upon absorption of light their energy is rapidly transferred to longer conjugated segments. In the presence of graphene the suppression of energy transfer results in preferential quenching of the longer wavelength components as they no longer are excited by energy transfer from neighboring shorter chains. The emission from shorter segments, which never had a component due to exciton migration, while quenched, are less severely affected.

## 5. Conclusions

In summary, we have demonstrated (1) that the presence of a nearby 2D quencher is shown to not just reduce the intensity of photoluminescence but also to reduce the PL lifetime, suppress emission at longer wavelengths preferentially and modify the effects of photo-bleaching and (2) that controlled quenching of photoluminescence by a 2D material such as graphene can be used to help understand energy transfer within individual conjugated polymers. In the case of the specific conjugated polymer investigated here, MEH-PPV, this dramatic change in PL is due to the suppression of energy transfer along the polymer backbone suggesting that the rate of intrachain energy transfer or exciton migration along the polymer backbone is  $k_{intra} \sim 2 \pm 1 \text{ ns}^{-1}$ .

## Acknowledgments

JDW would like to thank Professor Jui-Hung Hsu for useful discussions and use of equipment. We acknowledge support

from Ministry of Science and Technology, Taiwan projects 104-2112-M-155-001 and 106-2112-M-008-003-MY3.

## ORCID iDs

Xuan Long Ho  <https://orcid.org/0000-0002-8639-2417>

Po-Jui Chen  <https://orcid.org/0000-0001-6561-9224>

Wei-Yen Woon  <https://orcid.org/0000-0001-7299-9122>

Jonathon David White  <https://orcid.org/0000-0002-2250-1629>

## References

- [1] Salema A M S, El-Sheikha S M, Harraza F A, Ebrahimb S, Soliman M, Hafez H S, Ibrahim I A and Abdel-Mottaleb M S A 2017 Inverted polymer solar cell based on MEH-PPV/PC61BM coupled with ZnO nanoparticles as electron transport layer *Appl. Surf. Sci.* **425** 156–63
- [2] Prasad N, Singha I, Kumari A, Madhwal D, Madan S, Dixit S K, Bhatnagar P K and Mathur P C 2015 Improving the performance of MEH-PPV based light emitting diode by incorporation of graphene nanosheets *J. Lumin.* **159** 166–70
- [3] Hou L, Adhikari S, Tian Y, Scheblykin I G and Orrit M 2017 Absorption and quantum yield of single conjugated polymer poly[2-methoxy-5-(2-ethylhexyloxy)-1,4-phenylenevinylene] (MEH-PPV) molecules *Nano Lett.* **17** 1575
- [4] Hader K, Consani C, Brixner T and Engel V 2017 Mapping of exciton–exciton annihilation in MEH-PPV by time-resolved spectroscopy: experiment and microscopic theory *Phys. Chem. Chem. Phys.* **19** 31989
- [5] Hu Z, Shao B, Geberth G T and Vanden Bout D A 2018 Effects of molecular architecture on morphology and photophysics in conjugated polymers: from single molecules to bulk *Chem. Sci.* **9** 1101
- [6] Chang R et al 2000 Experimental and theoretical investigations of absorption and emission spectra of the light-emitting polymer MEH-PPV in solution *Chem. Phys. Lett.* **317** 142
- [7] Hu D, Yu J, Wong K, Bagchi B, Rossky P J and Barbara P F 2007 Collapse of stiff conjugated polymers with chemical defects into ordered, cylindrical conformations *Nature* **405** 1030
- [8] Nguyen T-Q, Wu J, Tolbert S H and Schwartz B J 2001 Control of energy transport in conjugated polymers using an ordered mesoporous silica matrix *Adv. Mater.* **13** 609
- [9] Hu Z, Adachi T, Haws R, Shuang B, Ono R J, Bielawski C W, Landes C F, Rossky P J and Vanden Bout D A 2014 Excitonic energy migration in conjugated polymers: the critical role of interchain morphology *J. Am. Chem. Soc.* **136** 16023
- [10] Lim T-S, Hsiang J-C, White J D, Hsu J H, Fan Y L, Lin K F and Fann W S 2007 Single short-chain conjugated polymer studied with optical spectroscopy: a donor-accepter system *Phys. Rev. B* **75** 165204
- [11] Huser T and Yan M 2001 Solvent-related conformational changes and aggregation of conjugated polymers studied by single molecule *J. Photochem. Photobiol. A* **144** 43
- [12] Lee Y J, Kim D Y and Barbara P F 2006 Effect of sample preparation and excitation conditions on the single molecule spectroscopy of conjugated polymers *J. Phys. Chem. B* **110** 9739–42
- [13] Swathi R S and Sebastian K L 2009 Long range resonance energy transfer from a dye molecule to graphene has (distance)–4 dependence *J. Chem. Phys.* **130** 086101

- [14] Federspiel F et al 2015 Distance dependence of the energy transfer rate from a single semiconductor nanostructure to graphene *Nano Lett.* **15** 1252–8
- [15] Jaemyung K, Cote L J, Kim F and Huang J 2010 Visualizing graphene based sheets by fluorescence quenching microscopy *J. Am. Chem. Soc.* **132** 260–7
- [16] Kasry A, Ardakani A A, Tulevski G S, Menges B, Copel M and Vyklicky L 2012 Highly efficient fluorescence quenching with graphene *J. Phys. Chem. C* **116** 2858
- [17] Vasilev K, Knoll W and Kreiter M 2004 Fluorescence intensities of chromophores in front of a thin metal film *J. Chem. Phys.* **120** 3439
- [18] Wang Y, Kurunthu D, Scott G W and Bardeen C J 2010 Fluorescence quenching in conjugated polymers blended with reduced graphitic oxide *J. Phys. Chem. C* **114** 4153–9
- [19] Ran C, Wang M, Gao W, Ding J, Shi Y, Song X, Chen H and Ren Z 2012 Study on photoluminescence quenching and photostability enhancement of MEH-PPV by reduced graphene oxide *J. Phys. Chem. C* **116** 23053–60
- [20] Yeltik A, Kucukayan-Dogu G, Guzelurk B, Fardindoost S, Kelestemur Y and Demir H V 2013 Evidence for nonradiative energy transfer in graphene-oxide-based hybrid structures *J. Phys. Chem. C* **117** 25298
- [21] Chuang M C and Woon W-Y 2016 Nucleation and growth dynamics of graphene on oxygen exposed copper substrate *Carbon* **103** 384–90
- [22] Giustiniano C T C F, Martin-Fernandez I, Andersen H, Balakrishnan J and Özyilmaz B 2015 ‘Bubble-Free’ electrochemical delamination of CVD graphene films *Small* **11** 189–94
- [23] Ennis D, Betz H and Ade H 2006 Direct spincoating of polystyrene thin films onto poly(methyl methacrylate) *J. Polym. Sci. B* **44** 3234–44
- [24] Liang J J, Hsu J H, Lim T S and White J D 2010 Photophysics of single PPV derivative polymers *J. Chin. Chem. Soc.* **57** 478–89
- [25] Becker W 2012 Fluorescence lifetime imaging—techniques and applications *J. Microsc.* **247** 119–36
- [26] Liang J-J, White J D, Chen Y C, Wang C F, Sun W Y, Hsu J H, Fann W S, Peng K Y and Chen S A 2006 Heterogeneous energy landscapes of individual luminescent conjugated polymers *Phys. Rev. B* **74** 085209
- [27] Rassamesard A et al 2009 Environmental effect on the fluorescence lifetime and quantum yield of single extended luminescent conjugated polymers *J. Phys. Chem. C* **113** 18681–8
- [28] Hofmann F J, Vogelsang J and Lupton J M 2016 Impact of charge carrier injection on single-chain photophysics of conjugated polymers *Appl. Phys. Lett.* **108** 263301
- [29] Ho X L, Chen P-J, Woon W-Y and White J D 2017 Fluorescence lifetime, dipole orientation and bilayer polymer films *Chem. Phys. Lett.* **686** 212–7
- [30] Kohler B E and Samuel I D W 1995 Experimental determination of conjugation lengths in long polyene chains *J. Chem. Phys.* **103** 6248
- [30] Kohler B E and Woehl J C 1995 A simple model for conjugation lengths in long polyene chains *J. Chem. Phys.* **103** 6253
- [31] Wang C F, White J D, Lim T L, Hsu J H, Yang S C, Fann W S, Peng K Y and Chen S A 2003 Illumination of exciton migration in rod-like luminescent conjugated polymers by single molecule spectroscopy *Phys. Rev. B* **67** 035202
- [32] Rossi G, Chance R R and Silbey R 1989 Conformational disorder in conjugated polymers *J. Chem. Phys.* **90** 7594
- [33] Nguyen T Q, Wu J, Doan V and Schwartz B J 2000 Control of energy transfer in oriented conjugated polymer-mesoporous silica composites *Science* **288** 652
- [34] Sun W-Y, Yang S-C, White J D, Hsu J-H, Peng K-Y, Chen S A and Fann W S 2005 Conformation and energy transfer in a single luminescent conjugated polymer *Macromolecules* **38** 2966–73
- [35] Burrows H D, Seixas de Melo J, Serpa C, Arnaut L G, da G. Miguel M, Monkman A P, Hamblett I and Navaratnam S 2002 Triplet state dynamics on isolated conjugated polymer chains *Chem. Phys.* **285** 3
- [36] Barbara P F, Gesquiere A J, Park S-J and Lee Y J 2005 Single-molecule spectroscopy of conjugated polymers *Acc. Chem. Res.* **38** 602
- [37] Nothaft M, Hohla S, Jelezko F, Pflaum J and Wrachtrup J 2012 The role of oxygen-induced processes on the emission characteristics of single molecule emitters *Phys. Status Solidi b* **249** 661–5